Japanese Journal of Applied Physics **55**, xxxxxx (2016)
http://doi.org/**10.7567/JJAP.55.xxxxxx**

REGULAR PAPER

JJAP PROOF

Production characteristics of reactive oxygen/nitrogen species in water using atmospheric pressure discharge plasmas

Kazuhiro Takahashi[1]*, Kohki Satoh[1], Hidenori Itoh[1], Hideki Kawaguchi[1], Igor Timoshkin[2], Martin Given[2], and Scott MacGregor[2]

[1]*Muroran Institute of Technology, Muroran, Hokkaido 050-8585, Japan*
[2]*University of Strathclyde, Glasgow G1 1XW, U.K.*

*E-mail: ktakahashi@mmm.muroran-it.ac.jp

Received November 30, 2015; revised January 27, 2016; accepted February 13, 2016; published online xxxx yy, zzzz

A pulsed discharge, a DC corona discharge, and a plasma jet are separately generated above a water surface, and reactive oxygen species and reactive nitrogen species (ROS/RNS) in the water are investigated. ROS/RNS in water after the sparging of the off-gas of a packed-bed dielectric barrier discharge (PB-DBD) are also investigated. H_2O_2, NO_2^-, and NO_3^- are detected after plasma exposure and only NO_3^- after off-gas sparging. Short-lifetime species in plasma are found to play an important role in H_2O_2 and NO_2^- production and long-lifetime species in NO_3^- production. NO_x may inhibit H_2O_2 production through OH consumption to produce HNO_2 and HNO_3. O_3 does not contribute to ROS/RNS production. The pulsed plasma exposure is found to be effective for the production of H_2O_2 and NO_2^-, and the off-gas sparging of the PB-DBD for the production of NO_3^-. © 2016 The Japan Society of Applied Physics

1. Introduction

In recent years, the study of plasma in contact with water has gained increasing attention and the water is known as plasma-treated water (PTW; also called plasma-activated medium, plasma-activated water, and so on). PTW is produced by various types of discharge plasma such as gliding arc,[1–3] plasma jet,[4–6] and dielectric barrier discharge.[7,8] In general, many kinds of species, such as radicals, ions, and ozone (O_3), are produced in plasma, and some of the species in the plasma in contact with water act as precursors of reactive oxygen species and reactive nitrogen species (ROS/RNS) in water.

PTW containing the ROS/RNS is applied to various fields such as disinfection,[1,3–5,7,8] agriculture,[2,9] and plasma medicine.[6] Several groups suggested that hydrogen peroxide (H_2O_2), peroxynitrous acid (HOONO), nitrite (NO_2^-), nitric acid (HNO_3), and/or synergistic effects between these species in water play a key role in bacterial inactivation, plant germination and growth, and chemical and biological effects. Naïtali et al.[1] reported that PTW and acidified water, containing 0.01 mmol/L H_2O_2, 1.6 mmol/L NO_2^-, and 0.13 mmol/L nitrate (NO_3^-), show a lethal effect on *Hafnia alvei*. Kim et al.[3] found that PTW containing 2.94 mmol/L H_2O_2 contributes to 5-log reduction for *Escherichia coli*. Takaki[9] reported that water containing 0.12 mmol/L NO_3^- contributes to the improvement of the growth rate of *Brassica rapa* var. *perviridis*. Furthermore, Matsui et al.[10] also suggested that long-lifetime neutral particles in the gas phase, such as O_3, H_2O_2, and HNO_3, and synergistic effects between these species play a key role in the disinfection of *Geobacillus stearothermophilus* spores. To utilize the PTW effectively and efficiently, it is important to control the ROS/RNS concentration and to clarify the interaction between species in plasma and ROS/RNS in water as well as to investigate efficacy in the application fields, since PTW with a wide-ranging ROS/RNS concentration is used for the investigation of efficacy. Various types of discharge plasma can produce the ROS/RNS; however, few studies have focused on the correlation between the discharge plasma and the ROS/RNS as far as we know.

In this work, we generated a pulsed discharge, a DC corona discharge, an atmospheric pressure plasma jet, and a packed-bed dielectric barrier discharge (PB-DBD) as a plasma source to produce ROS/RNS in water. We exposed deionized water to the pulsed discharge, DC corona discharge, or plasma jet. We also sparged the off-gas of the PB-DBD into deionized water. Then, we investigated the concentration and production efficiency of the ROS/RNS in the water.

2. Experimental procedure

2.1 Pulsed discharge

The experimental apparatus for a pulsed discharge is similar to that used in a previous work.[11] A needle electrode and a water bath electrode were placed in a cylindrical discharge chamber to generate the pulsed discharge. The needle electrode was a stainless-steel nail with a diameter of 1.5 mm and a length of 19 mm, the water bath electrode was made of stainless steel with an inner diameter of 119 mm, a depth of 12 mm, and a capacity of 0.13 L, and the cylindrical chamber was made of acrylic resin with an inner diameter of 140 mm, a height of 100 mm, and a capacity of 1.54 L. Deionized water of 100 mL was poured into the water bath electrode, and the distance between the tip of the needle electrode and the water surface was fixed at 4 mm. Ar, N_2, O_2, or a gas mixture of Ar/O_2, N_2/O_2, or Ar/N_2 was used as a background (BG) gas, and fed into the chamber at a constant flow rate of 5 L/min. The gas mixture ratios were Ar/O_2, N_2/O_2, and $Ar/N_2 = 80/20$, 60/40, 40/60, and 20/80%.

A pulsed high voltage with a pulse width of 500 ns generated by a Blumlein generator, which has two coaxial transmission lines (Fujikura 5D-2V) with a length of 50 m and a capacitance of 5 nF, was applied to the needle electrode to generate the pulsed discharge above the water surface. The coaxial transmission lines were charged to a negative voltage of 14.14 kV, and the pulse repetition rate was 20 pps (pulse per second). The applied voltage was measured using a high-voltage probe (Iwatsu Test Instruments HV-P30) and the discharge current was obtained by measuring the voltage drop across a non-inductive resistor connected in series

 © 2016 The Japan Society of Applied Physics

JJAP PROOF

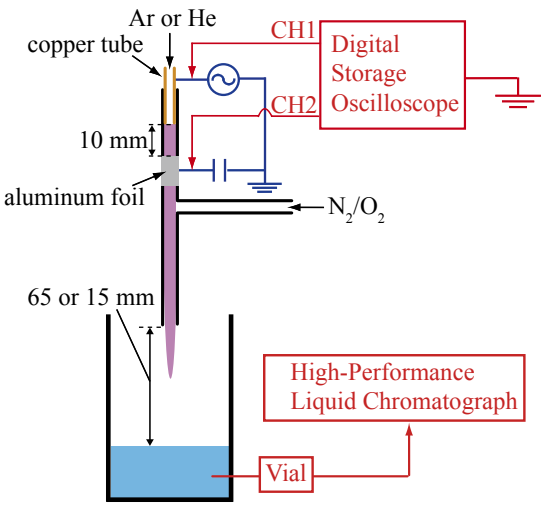

Fig. 1. (Color online) Schematic diagram of experimental apparatus for plasma jet.

between the bath electrode and the ground. The input power was calculated by multiplying the applied voltage and discharge current, and the input energy was obtained from the time integration of the input energy. Water samples of 1.2 mL were taken after plasma exposure and analyzed using a high-performance liquid chromatograph (HPLC; Shimadzu Prominence) equipped with an ion chromatography column (Shodex IC NI-424) in combination with an autosampler. The eluent of the HPLC was a mixed solution of 3 mmol/L acetic acid and 1.9 mmol/L potassium hydroxide, and the wavelength of the absorbance detector was fixed at 220 nm.

2.2 Corona discharge

The experimental apparatus for a corona discharge is similar to that used in a previous work.[12] A comb-shaped electrode and a plastic container were placed in an acrylic discharge chamber with a length of 140 mm, a width of 260 mm, and a height of 100 mm. The comb-shaped electrode consisted of four clusters, each of which has 26 (13×2) combs, with a width of 1.6 mm and a length of 15 mm, placed at intervals of 4 mm. Deionized water of 100 mL was poured into the container, and the distance between the tip of the electrode and the water surface was fixed at 15 mm. An aluminum foil was immersed into the water and earthed. A gas mixture of N_2/O_2 or Ar/O_2 was used as a BG gas and fed into the chamber at a constant flow rate of 2 L/min. The BG gas mixture ratios were $Ar/O_2 = 80/20$, 60/40, and 40/60%, and $N_2/O_2 = 60/40$ and 40/60%. A positive DC high voltage of 14.7–15.4 kV was applied to the electrode to generate a corona discharge between the electrode and the water surface, with an input power of 6 W. The input energy was obtained from the time integration of the input power. Water samples of 1.2 mL were analyzed using the HPLC after plasma exposure.

2.3 Plasma jet

Figure 1 shows a schematic diagram of the experimental apparatus for the plasma jet. The atmospheric pressure plasma jet reactor consisted of a T-shaped glass tube, a copper tube, and an aluminum sheet. The copper tube was inserted into an end of the main tube of the T-shaped glass tube, and the aluminum sheet was bound around the main tube and earthed. The gap length between the copper tube and the aluminum sheet was fixed at 10 mm. An Ar or He gas was fed into the main tube through the copper tube at a constant flow rate of 10 or 5 L/min, respectively. A gas mixture of N_2/O_2, the mixture ratio of which is $N_2/O_2 =$ 100/0, 80/20, 60/40, 40/60, 20/80, and 0/100%, was mixed into the plasma jet from the side tube of the T-shaped glass tube at a constant flow rate of 0.1 L/min.

An AC high voltage of 6.0–7.0 kV amplitude generated by a neon-sign transformer (Kodera Electronics CR-N16) was applied to the copper tube to generate the plasma jet. The input power was calculated by the Lissajous figure method,[13] and the input energy was obtained from the time integration of the input power. The applied voltage was measured using a high-voltage probe (Tektronix P6015A), and the charge amount was obtained by measuring the voltage drop across a ceramic capacitor with a capacitance of 10 nF, connected in series between the aluminum sheet and the ground. The voltage drop was measured using a high-voltage differential probe (GW Instek GDP-100). Deionized water of 200 mL was poured into a beaker placed below the plasma jet. The distance between the water surface and the outlet end of the main tube was fixed at 65 or 15 mm. The Ar gas flow rate was fixed at 5 L/min when the distance was fixed at 15 mm. The water was exposed to the plasma jet, and then water samples of 1.2 mL were taken and analyzed using the HPLC after plasma exposure.

2.4 Packed-bed dielectric barrier discharge

The experimental apparatus for a packed-bed dielectric barrier discharge (PB-DBD) is similar to that used in a previous work.[14] A PB-DBD reactor consisted of a glass tube filled with soda-lime glass balls, an inner rod electrode, and an outer mesh electrode. The diameters of the glass tube, glass balls, and rod electrode were 22, 3.0, and 2.0 mm, respectively. Ar, N_2, O_2, or a gas mixture of Ar/O_2, N_2/O_2, or Ar/N_2 was used as a BG gas and fed into the reactor at a constant flow rate of 2 L/min. The gas mixture ratios were Ar/O_2, N_2/O_2, and $Ar/N_2 = 80/20$, 60/40, 40/60, and 20/80%.

A sinusoidal high voltage of 5.7–12.0 kV amplitude generated by the neon-sign transformer was applied between electrodes to generate the PB-DBD. The input energy was obtained from the time integration of input power calculated by the Lissajous figure method. The off-gas from the reactor was introduced through a Teflon tube with a length of 60 cm and an inner diameter of 3.96 mm and sparged into deionized water of 100 mL in a flask. Water samples of 1.2 mL were taken and analyzed using the HPLC after off-gas sparging. Furthermore, the PB-DBD off-gas was analyzed using a Fourier transform infrared spectrophotometer (JASCO FT/IR-4200) equipped with a gas cell (Infrared Analysis 10-PA), which has an optical path length of 10 m.

3. Results and discussion

In HPLC analysis, H_2O_2, NO_2^-, and NO_3^- were detected in the sampled water. Figure 2 shows the H_2O_2 concentrations in the sampled water as functions of specific energy, which is defined as the input energy per unit volume of water. H_2O_2 was produced in the cases of pulsed discharge, corona discharge, and plasma jet, but not in the case of PB-DBD off-gas sparging; therefore, short-lifetime active and/or energetic

 © 2016 The Japan Society of Applied Physics

JJAP PROOF

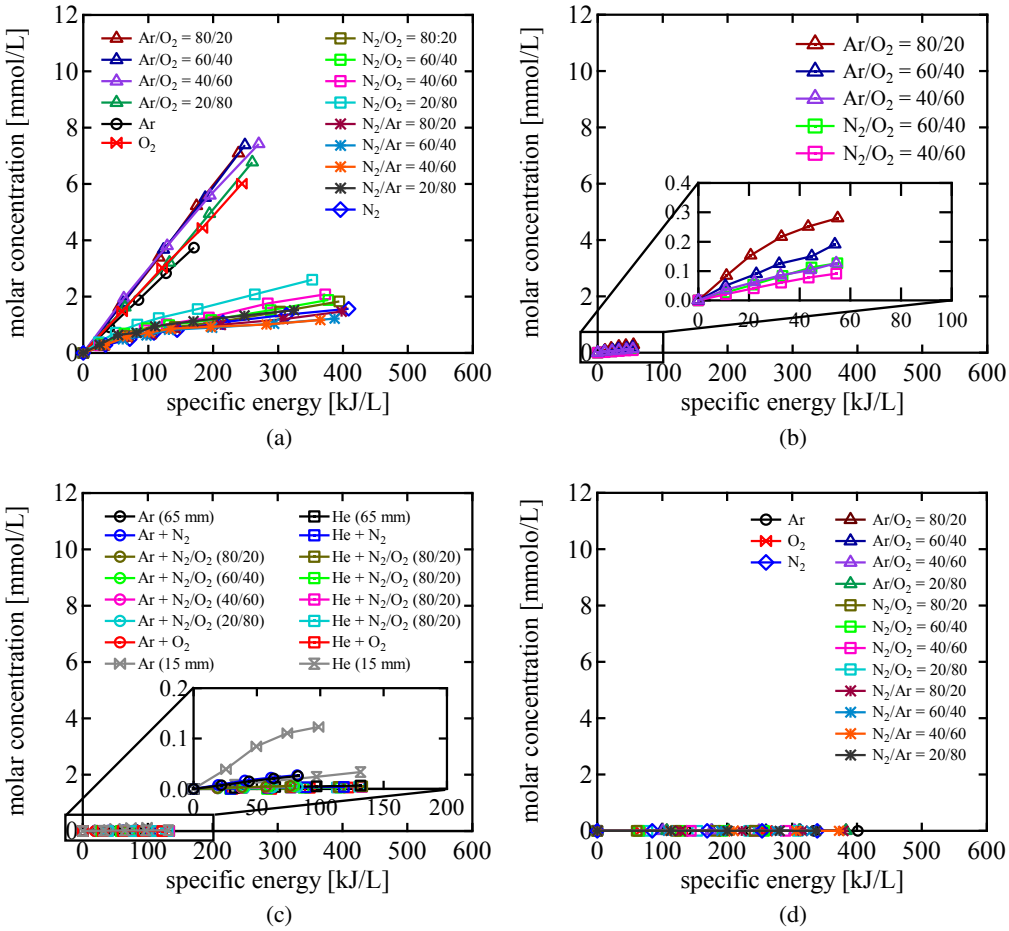

Fig. 2. (Color online) H_2O_2 concentrations in sampled water as functions of specific energy: (a) pulsed discharge, (b) corona discharge, (c) plasma jet, and (d) PB-DBD.

species in the plasma in contact with water probably contribute to H_2O_2 production. When water is exposed to plasma, vaporized water molecules can be dissociated as follows:[15–17]

$$H_2O + e \rightarrow OH + H + e, \quad (1)$$

$$H_2O + e \rightarrow H_2O^+ + 2e, \quad (2)$$

$$H_2O^+ + H_2O \rightarrow H_3O^+ + OH. \quad (3)$$

Then, H_2O_2 can be produced from OH radicals represented as[18,19]

$$OH + OH \rightarrow H_2O_2 \quad (k = 1.5 \times 10^{-11}\ cm^3 \cdot mol^{-1} \cdot s^{-1}), \quad (4)$$

where k is the rate constant. Although water vapor is contained within the concentration of 20 ppm as impurities in the BG gas of the PB-DBD, the concentration of OH radicals can be quite small, so that H_2O_2 produced by the reaction shown by Eq. (4) is negligible.

H_2O_2 concentrations in the pulsed discharge monotonically increased with the specific energy, while the amount of H_2O_2 in the BG gas containing N_2 was found to be smaller than that in the other BG gas. This may be due to the inhibition of H_2O_2 production by species containing N atom(s). The H_2O_2 production efficiency of 31.2 µmol/kJ at a maximum was obtained when an Ar/O_2 mixture was used. The H_2O_2 concentrations in the corona discharge tended to increase with Ar or N_2 content in the mixture gas, and the maximum H_2O_2 production efficiency of 7.6 µmol/kJ was obtained in $Ar/O_2 = 80/20\%$. When the plasma jet was used, the amount of H_2O_2 was small and slightly increased with the shortening of the distance between the plasma and the water surface. The H_2O_2 production efficiency in Ar without the N_2/O_2 mixture was 1.7 µmol/kJ, which is significantly lower than that in pulsed discharge. Van Gils et al.[5] investigated the H_2O_2 concentrations in water exposed to an Ar plasma jet, and reported that the H_2O_2 production efficiency was 0.7 µmol/kJ at a maximum. This value differs slightly from the efficiency of this work, so that pulsed discharge may be suitable for highly efficient H_2O_2 production.

Figure 3 shows the NO_2^- concentrations in the sampled water as functions of specific energy. NO_2^- was produced by exposure to the pulsed discharge, corona discharge, and plasma jet when the BG gas contained N_2, but not by the sparging of the PB-DBD off-gas; therefore, short-lifetime active and/or energetic species in the plasma in contact with water probably contribute to NO_2^- production. Furthermore, the NO_2^- concentration in the pulsed discharge was found to increase and then decrease with the increase in specific energy. When water is exposed to plasma in the BG gas containing N_2, the following reactions[20] can occur:

$$N_2 + e(fast) \rightarrow 2N + e(slow), \quad (5)$$

$$N + OH \rightarrow NO + H \quad (k = 4.9 \times 10^{-11}\ cm^3 \cdot mol^{-1} \cdot s^{-1}), \quad (6)$$

$$NO + OH + M \rightarrow HNO_2 + M \quad (k = 7.4 \times 10^{-31}\ cm^6 \cdot mol^{-2} \cdot s^{-1}), \quad (7)$$

 © 2016 The Japan Society of Applied Physics

JJAP PROOF

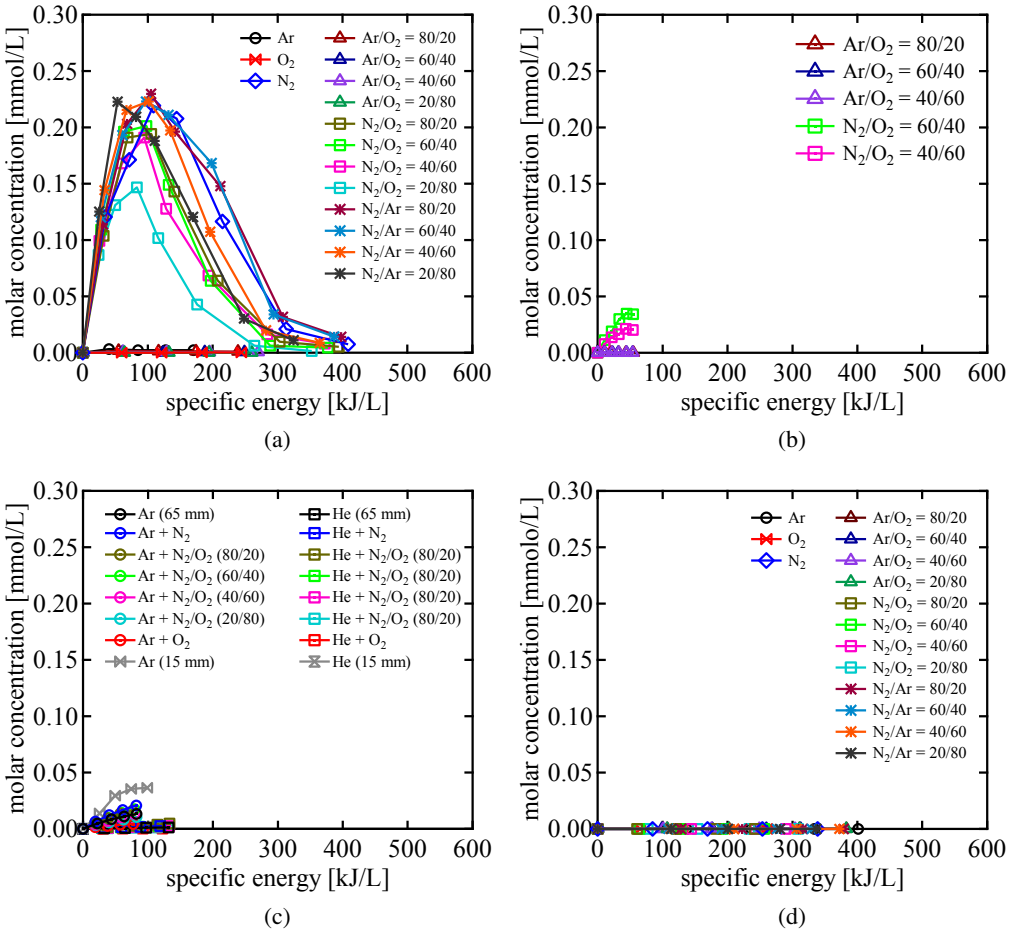

Fig. 3. (Color online) NO_2^- concentrations in sampled water as functions of specific energy: (a) pulsed discharge, (b) corona discharge, (c) plasma jet, and (d) PB-DBD.

where M is the third body. Then, HNO_2 dissolves in water and dissociates into NO_2^- and H^+ in acid-base equilibrium ($pK_a = 3.3$) represented by[5,21]

$$HNO_2 \rightleftarrows NO_2^- + H^+. \quad (8)$$

Furthermore, HNO_2 reacts with H_2O_2 to form HOONO by[5,22]

$$HNO_2 + H_2O_2 \rightarrow HOONO + H_2O. \quad (9)$$

HOONO is an unstable species and rapidly turns into NO_3^- and H^+.[22]

$$HOONO \rightarrow NO_3^- + H^+. \quad (10)$$

In this work, the pH drop of the water after pulsed discharge exposure was observed, and the pH decreased below 4.0 after 5 min exposure (corresponding to a specific energy of 32 kJ/L) and 3.0 after 30 min exposure (corresponding to a specific energy of 208 kJ/L) in $N_2/O_2 = 80/20\%$. Therefore, NO_2^- in the water may be converted into NO_3^- through the reactions shown by Eqs. (8)–(10), resulting in the drop of the NO_2^- concentration with the increase in specific energy. NO_2^- concentrations in the corona discharge and plasma jet showed a tendency to saturate, and this result is also probably due to the drop in the pH of the water. The maximum NO_2^- production efficiency of 5.0 μmol/kJ was obtained using the pulsed discharge in $N_2/Ar = 20/80\%$ at the specific energy of 25 kJ/L.

In the PB-DBD, the BG gas contains water vapor within the concentration of 20 ppm as impurities, and the concentration is six orders of magnitude lower than that of N_2. OH radicals can be produced from a trace of water vapor, but the concentration of OH radicals can be much lower than that of N atoms produced from N_2 in the PB-DBD; therefore, the reaction shown by Eq. (4) can be negligible and the reactions shown by Eqs. (6) and (7) can occur. However, NO_2^- was not detected, so that the concentration of NO_2^- in the water was below the detection limit (20 nmol/L) or NO_2^- was rapidly converted into other species.

Figure 4 shows the NO_3^- concentrations in the sampled water as functions of specific energy. When water is exposed to plasma in the BG gas containing N_2, the following reactions[18,23] may occur in addition to the reactions shown by Eqs. (5)–(7):

$$NO + O + M \rightarrow NO_2 + M \quad (k = 8.9 \times 10^{-32}\ cm^6 \cdot mol^{-2} \cdot s^{-1}), \quad (11)$$

$$NO_2 + OH + M \rightarrow HNO_3 + M \quad (k = 2.6 \times 10^{-30}\ cm^6 \cdot mol^{-2} \cdot s^{-1}). \quad (12)$$

Then, HNO_3 dissolves in water and completely dissociates into NO_3^- and H^+. The reactions shown by Eqs. (8)–(10) also contribute to NO_3^- production. Furthermore, the production of HNO_2 and HNO_3 by the reactions shown by Eqs. (7) and (12) causes OH consumption, so that H_2O_2

 © 2016 The Japan Society of Applied Physics

JJAP PROOF

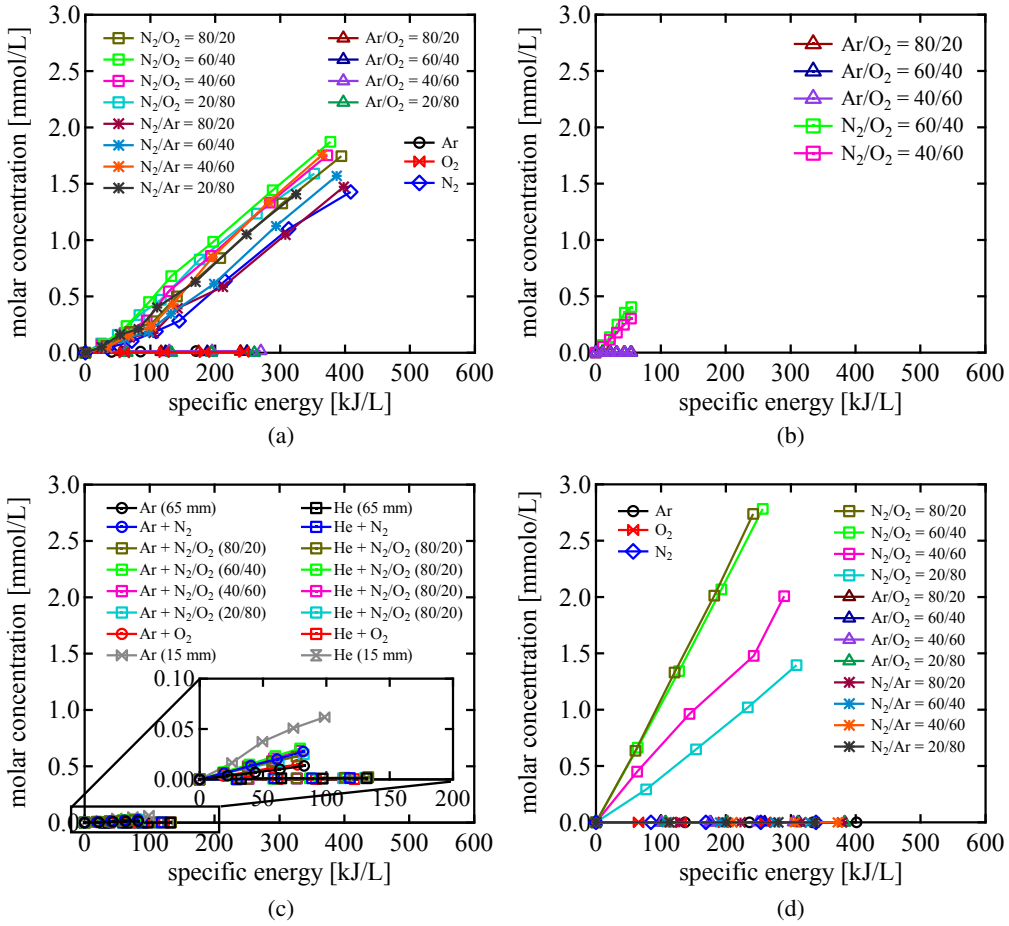

Fig. 4. (Color online) NO_3^- concentrations in sampled water as functions of specific energy: (a) pulsed discharge, (b) corona discharge, (c) plasma jet, and (d) PB-DBD.

production by the reaction shown by Eq. (4) is inhibited, resulting in the decrease in the H_2O_2 amount in the BG gas containing N_2.

NO_3^- was also produced by off-gas sparging. In the PB-DBD, a trace of OH radicals is produced from water vapor contained in the BG gas as impurities, as described above, so that the reaction shown by Eq. (12) has little contribution to HNO_3 production. Thus, other reactions by long-lifetime species to produce NO_3^- may occur in off-gas sparging. The NO_3^- concentrations in the pulsed discharge monotonically increased with the specific energy, and the NO_3^- production efficiency of 5.1 µmol/kJ was obtained at a maximum. In the corona discharge, NO_3^- tended to increase with Ar or N_2 content in the mixture gas, and the NO_3^- production efficiency of 8.0 µmol/kJ was obtained. When the plasma jet was used, the amount of NO_3^- was small and slightly increased with N_2 mixing. In the case of off-gas sparging, NO_3^- was produced in the N_2/O_2 mixture and its amount was found to increase with N_2 content. The maximum NO_3^- production efficiency of 11.3 µmol/kJ was obtained in $N_2/O_2 = 80/20\%$.

Figure 5 shows the absorbance spectra of the PB-DBD off-gas before and after sparging, obtained by infrared absorption spectroscopy. Absorption peaks corresponding to nitrous oxide (N_2O; 2224 cm^{-1}),[24] dinitrogen pentaoxide (N_2O_5; 1247, 1704, and 1745 cm^{-1}),[25] HNO_3 (1312, 1346, and 1698 cm^{-1}),[26] and O_3 (1042 cm^{-1})[27] were detected in the N_2/O_2 mixture. It was suggested above that a trace of NO_2^- might be produced in water via the reaction shown by Eq. (7); however, NO_2^- was not detected. O_3 was observed in the off-gas as shown in Fig. 5 and O_3 can dissolve in water; therefore, the reaction shown by Eq. (13) can occur.[28]

$$NO_2^- + O_3 \rightarrow NO_3^- + O_2. \quad (13)$$

Furthermore, considering that NO_2^- was not detected, the rate of reaction can be sufficiently high.

It was described that a trace of HNO_3 is produced via the reaction shown by Eq. (12). In addition, HNO_3 may also be produced by the reaction shown by Eq. (14),[18] since N_2O_5 and water vapor are contained in the off-gas before sparging, as shown in Fig. 5.

$$N_2O_5 + H_2O \rightarrow 2HNO_3. \quad (14)$$

The intensities of absorption peaks corresponding to N_2O_5 and HNO_3 were reduced by sparging, while there were little changes in the intensities of absorption peaks corresponding to N_2O and O_3. This indicates that HNO_3 in the off-gas dissolves in water and HNO_3 is produced in liquid phase by the reaction shown by Eq. (14), contributing to NO_3^- production, and that N_2O and O_3 do not produce ROS/RNS in water.

 © 2016 The Japan Society of Applied Physics

JJAP PROOF

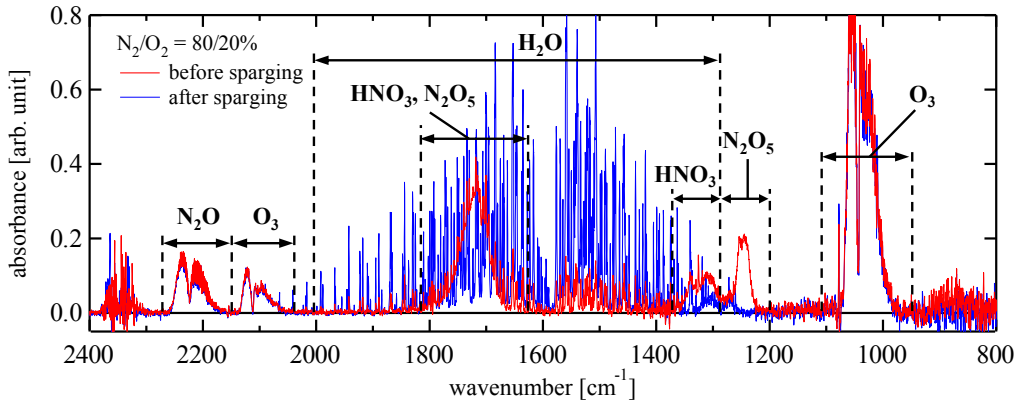

Fig. 5. (Color online) Absorbance spectra of PB-DBD off-gas before and after sparging.

4. Conclusions

We have investigated reactive oxygen species and reactive nitrogen species (ROS/RNS) in water, exposed directly to a pulsed discharge, a DC corona discharge, and a plasma jet or sparged the off-gas of a packed-bed dielectric barrier discharge (PB-DBD). H_2O_2, NO_2^-, and NO_3^- are produced after plasma exposure and only NO_3^- after off-gas sparging. Short-lifetime species in plasma such as OH radicals act as the precursors of H_2O_2 and NO_2^-, and long-lifetime species including N_2O_5 act as the precursor of NO_3^-. NO_x may inhibit H_2O_2 production through OH consumption to produce HNO_2 and HNO_3. O_3 is found not to be the precursor of ROS/RNS. In this work, the highest production efficiencies of H_2O_2 and NO_2^- are obtained to be 31.2 and 5.0 µmol/kJ, respectively, by pulsed-plasma exposure, and that of NO_3^- is obtained to be 11.3 µmol/kJ by the off-gas sparging of the PB-DBD.

Acknowledgment

This work is partially supported by The Royal Society International Exchanges Scheme.

1) M. Naïtali, G. Kamgang-Youbi, J.-M. Herry, M.-N. Bellon-Fontaine, and J.-L. Brisset, Appl. Environ. Microbiol. **76**, 7662 (2010).
2) D. P. Park, K. Davis, S. Gilani, C.-A. Alonzo, D. Dobrynin, G. Friedman, A. Fridman, A. Rabinovich, and G. Fridman, Curr. Appl. Phys. **13**, S19 (2013).
3) H.-S. Kim, K. C. Wright, I.-W. Hwang, D.-H. Lee, A. Rabinovich, A. Fridman, and Y. I. Cho, Int. Commun. Heat Mass Transfer **42**, 5 (2013).
4) Q. Zhang, Y. Liang, H. Feng, R. Ma, Y. Tian, J. Zhang, and J. Fang, Appl. Phys. Lett. **102**, 203701 (2013).
5) C. A. J. van Gils, S. Hofmann, B. K. H. L. Boekema, R. Brandenburg, and P. J. Bruggeman, J. Phys. D **46**, 175203 (2013).
6) S. Mohades, M. Laroussi, J. Sears, N. Barekzi, and H. Razavi, Phys. Plasmas **22**, 122001 (2015).
7) A. Kojtari, U. K. Ercan, J. Smith, G. Friedman, R. B. Sensenig, S. Tyagi, S. G. Joshi, H.-F. Ji, and A. D. Brooks, J. Nanomed. Biother. Discov. **4**, 120 (2013).
8) M. J. Traylor, M. J. Pavlovich, S. Karim, P. Hait, Y. Sakiyama, D. S. Clark, and D. B. Graves, J. Phys. D **44**, 472001 (2011).
9) K. Takaki, Dennetsu **51**, 64 (2012) [in Japanese].
10) K. Matsui, N. Ikenaga, and N. Sakudo, Jpn. J. Appl. Phys. **54**, 01AG06 (2015).
11) H. Shiota, H. Itabashi, K. Satoh, and H. Itoh, Electr. Eng. Jpn. **184** [1], 1 (2013).
12) Y. Itoh, K. Satoh, and H. Itoh, Denki Gakkai Ronbunshi A **132**, 807 (2012) [in Japanese].
13) H.-E. Wagner, R. Brandenburg, K. V. Kozlov, A. Sonnenfeld, P. Michel, and J. F. Behnke, Vacuum **71**, 417 (2003).
14) K. Takahashi, K. Satoh, and H. Itoh, IEEJ Trans. Fundam. Mater. **134**, 60 (2014).
15) Y. Itikawa and N. Mason, J. Phys. Chem. Ref. Data **34**, 1 (2005).
16) W. Lindinger, Phys. Rev. A **7**, 328 (1973).
17) R. P. Joshi and S. M. Thagard, Plasma Chem. Plasma Process. **33**, 17 (2013).
18) R. Atkinson, D. L. Baulch, R. A. Cox, J. N. Crowley, R. F. Hampson, R. G. Hynes, M. E. Jenkin, M. J. Rossi, and J. Troe, Atmos. Chem. Phys. **4**, 1461 (2004).
19) S. Mededovic and B. R. Locke, J. Phys. D **40**, 7734 (2007).
20) R. Atkinson, D. L. Baulch, R. A. Cox, R. F. Hampson, Jr., J. A. Kerr, and J. Troe, J. Phys. Chem. Ref. Data **18**, 881 (1989).
21) P. Lukes, E. Dolezalova, I. Sisrova, and M. Clupek, Plasma Sources Sci. Technol. **23**, 015019 (2014).
22) S. Goldstein, J. Lind, and G. Marényi, Chem. Rev. **105**, 2457 (2005).
23) L. D'Ottone, P. Campuzano-Jost, D. Bauer, and A. J. Hynes, J. Phys. Chem. A **105**, 10538 (2001).
24) T. Shimanouchi, *Tables of Molecular Vibrational Frequencies Consolidated* (National Bureau of Standards, Washington, D.C., 1972) Vol. I, p. 9.
25) E. L. Varetti and G. C. Pimentel, J. Chem. Phys. **55**, 3813 (1971).
26) W.-J. Chen, W.-J. Lo, B.-M. Cheng, and Y.-P. Lee, J. Chem. Phys. **97**, 7167 (1992).
27) T. Shimanouchi, J. Phys. Chem. Ref. Data **6**, 993 (1977).
28) S. A. Penkett, Nature **240**, 105 (1972).

 © 2016 The Japan Society of Applied Physics